

# Soft Matter

Accepted Manuscript

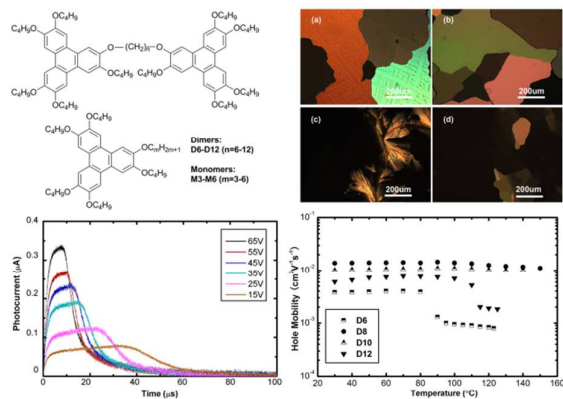


This is an *Accepted Manuscript*, which has been through the Royal Society of Chemistry peer review process and has been accepted for publication.

*Accepted Manuscripts* are published online shortly after acceptance, before technical editing, formatting and proof reading. Using this free service, authors can make their results available to the community, in citable form, before we publish the edited article. We will replace this *Accepted Manuscript* with the edited and formatted *Advance Article* as soon as it is available.

You can find more information about *Accepted Manuscripts* in the [Information for Authors](#).

Please note that technical editing may introduce minor changes to the text and/or graphics, which may alter content. The journal's standard [Terms & Conditions](#) and the [Ethical guidelines](#) still apply. In no event shall the Royal Society of Chemistry be held responsible for any errors or omissions in this *Accepted Manuscript* or any consequences arising from the use of any information it contains.



A clear structure-properties relationship was revealed in a series of triphenylene-based dimers, linkage length played an important role in the modulation of phase behaviors and charge carrier mobilities in discotic dimers.

## ARTICLE

# Modulation of phase behaviors and charge carrier mobilities by linkage length in discotic liquid crystal dimers

Cite this: DOI: 10.1039/x0xx00000x

Received 00th January 2012,

Accepted 00th January 2012

DOI: 10.1039/x0xx00000x

[www.rsc.org/](http://www.rsc.org/)

Yi-Fei Wang, Chun-Xiu Zhang\*, Hao Wu, Ao Zhang, Jian-Chuang Wang, Shuai-Feng Zhang and Jia-Ling Pu

A clear structure-properties relationship was revealed in a series of triphenylene-based dimers, which contained two triphenylene nuclei bearing five  $\beta$ -OC<sub>4</sub>H<sub>9</sub> substituents and linked through a flexible O(CH<sub>2</sub>)<sub>n</sub>O polymethylene chain (n=6-12). Dimers with the linkage close to twice the length of the free side chains (n=8, 9) exhibited a single Col<sub>hp</sub> phase, while others with linkage shorter (n=6, 7) or longer (n=10, 11, 12) showed multiphase with a transition from Col<sub>hp</sub> phase to Col<sub>h</sub> phase; Hole mobilities of Col<sub>hp</sub> phases reached  $1.4 \times 10^{-2} \text{cm}^2 \text{V}^{-1} \text{s}^{-1}$  in dimer for which the linkage is exactly twice the length of the free side chains (n=8), and decreased regularly both with linkage length becoming shorter or longer. This modulation of phase behaviors and charge carrier mobilities was demonstrated to be generated by various steric perturbations introduced by linkage with different length, which result in different degree of lateral fluctuation of discotic moieties in the columns.

## Introduction

Discotic liquid crystals are attractive flexible organic semiconductors due to their unique self-assembly nanostructure with remarkable charge carrier transport property.<sup>1</sup> The polymerization of discotic liquid crystal is an inevitable approach in their application in organic printed electronics, which demand materials with thermal stabilities as well as mechanical properties. Due to the  $\pi$ -stacking nature of columnar phases, minor changes in molecular structures can highly affect the packing structures and always result in uncontrollable phase behaviors and unpredictable transport properties after polymerization.<sup>2-4</sup> There are thus high needs for the understanding of the structure-properties relationship in discotic liquid crystal polymers.

Discotic liquid crystal Dimers serve as ideal model compounds for polymers or networks, due to the striking similarities in their transitional behaviors coupled with their ease of purification and characterization.<sup>5, 6, 7</sup> In our previous work, We have designed and synthesized a series of triphenylene-based dimers, each of triphenylene nuclei bears five  $\beta$ -OC<sub>4</sub>H<sub>9</sub> substituents, which are linked through the remaining  $\beta$ -positions by a flexible O(CH<sub>2</sub>)<sub>n</sub>O polymethylene chain (n=2-12).<sup>8</sup> These dimers were inclined to form a columnar plastic phase (Col<sub>hp</sub>), which is a highly ordered phase with a three-dimensional positional order, while maintaining the rotational mobility.<sup>8, 9, 10</sup> Besides its three-dimensional order, this phase is very closely related to the normal columnar phase (Col<sub>h</sub>) with no major differences in structure and dynamics, but charge mobility in columnar plastic phase can reach the order of  $10^{-2} \text{cm}^2 \text{V}^{-1} \text{s}^{-1}$  which is about an order of

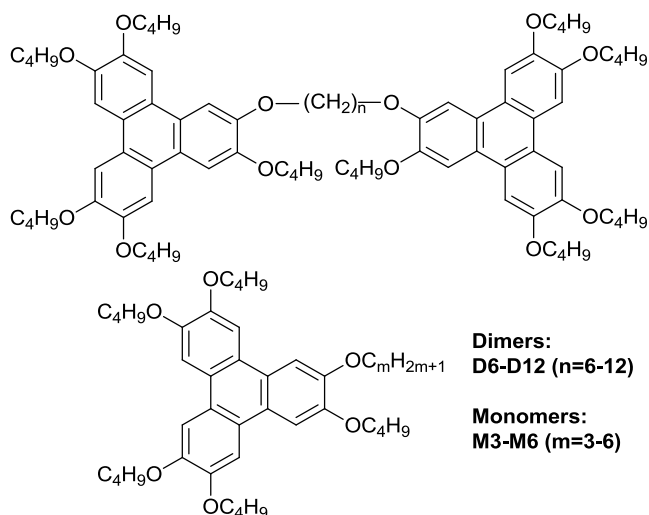
magnitude higher than that of normal columnar phase.<sup>8-11</sup> All these dimers **D6-D12** (Scheme 1) for which n>5 all gave the highly ordered Col<sub>hp</sub> phase. With the changes of linkage length, various ranges of the mesophase were observed in these dimers and several of them exhibited multiphase behaviors with transition from Col<sub>hp</sub> phases to Col<sub>h</sub> phases. These dimers thus provided us perfect models for studies of the connection between linkage lengths and properties.

To date, there are few works focus on linkage lengths in discotic dimers, especially their effects on phase behaviors and transport properties. In this work, phase behaviors and time-of-flight (TOF) mobilities of dimers **D6-D12** were investigated concerning their relevance on the linkage lengths. It was found that the dimers with linkage lengths close to twice of side chains (n=8, 9) exhibited single Col<sub>hp</sub> phases, while others with linkage shorter (n=6, 7) or longer (n=10, 11, 12) showed multiphase with transitions from Col<sub>hp</sub> phases to Col<sub>h</sub> phases. Hole mobilities under Col<sub>hp</sub> phases reached  $1.4 \times 10^{-2} \text{cm}^2 \text{V}^{-1} \text{s}^{-1}$  in dimer for which n=8 and decreased regularly both with linkage length becoming shorter or longer. In these types of dimers, as each of subunit was most likely to occupy neighboring two columns, a lateral correlation between the columns which we attribute to the steric perturbation was introduced by the linkages between them. Therefore, the various behaviors on phase transition and charge mobility of **D6-D12** can be attributed to different degree of lateral fluctuations of the disc-like units in columns caused by different steric perturbations.

To clarify these steric perturbations, we newly designed and synthesized monomers **M3-M6** (Scheme 1) by "halving" these dimers from their linkages. In the formations of columnar

phases, these monomers can be treated as the subunits of dimers with the restrictions between them having been cancelled. A prediction on phase behaviours of these monomers was made based on our investigation. Phase study results of these monomers by DSC, POM and XRD were completely consistent with the prediction, which confirmed our hypothesis on steric perturbation effect. The twice of side chain was demonstrated to be a perfect length for linkage of these dimers which endured the minimized steric perturbation. With linkage becoming shorter or longer, this perturbation increased and appeared as strain or steric crowd, respectively.

To further understand the relevance between the linkage length of dimers and their charge carrier mobility, hole mobilities of **M3-M6** were investigated by TOF method. The results were consistent with our above description on the existence of steric perturbation. Furthermore, a comparison on hole mobilities in  $\text{Col}_{\text{hp}}$  phase between dimers and their monomers also been made based on our measurement results. Our work provided a structure-property model in discotic dimer systems, which enable us to discuss the effect of steric perturbations introduced by linkage with different length and lateral fluctuation of discotic moieties in the columns.



**Scheme 1** Molecular structures of dimers **D6-D12** and the corresponding monomers **M3-M6**.

## Results and discussion

The phase behaviors of dimers **D6-D12** have been reported in our previous work and also summarized in Table 1.<sup>8</sup> Herein, we concerned on the phase behaviors and charge carrier mobilities of different dimers, and investigated their relevance on the linkage lengths.

It was clear from Table 1, dimers **D8** and **D9** for which the linkages were close to twice the lengths of the free side chains exhibited single columnar plastic phases. However, with the linkages becoming longer or shorter, dimers **D6**, **D7** and **D10-D12** all showed multiple phase behaviours, the highly ordered columnar plastic phases occurred at lower temperature region and transitioned into lower ordered  $\text{Col}_{\text{h}}$  at higher temperature regions. The phase transition temperatures of these dimers also changed regularly with changes of linkage lengths. Isotropic temperatures increased gradually from **D6** to **D8** and remained stable in **D9**, then decreased with the increasing of linkage lengths. The higher isotropic temperatures indicated more stable packing structure were formed in **D8** and **D9**. Transition

temperatures between  $\text{Col}_{\text{hp}}$  phase and  $\text{Col}_{\text{h}}$  phase in dimers with multiple phases showed similar behaviours, a step increasing was observed from **D6** to **D7** while the result of **D10** to **D12** was conversely. These interesting phenomena in phase behaviours and transition temperatures were rarely reported in discotic liquid crystal dimers, which indicated a clear relationship between packing structure and linkage length.

**Table 1** Phase behaviours of dimers **D6-D12**. Transition temperatures and enthalpies were based on the 1<sup>st</sup> cooling runs by DSC at  $10\text{ }^{\circ}\text{Cmin}^{-1}$  (I = isotropic phase;  $\text{Col}_{\text{h}}$  = hexagonal columnar phase;  $\text{Col}_{\text{hp}}$  = hexagonal columnar plastic phase).

Compound	Phase	$T/{}^{\circ}\text{C}(\Delta H/\text{Jg}^{-1})$	Phase <sup>a</sup>
<b>D6</b>	$\text{Col}_{\text{hp}}$	$\xleftarrow{81.8(-2.7)}$	$\text{Col}_{\text{h}}$
		$\xleftarrow{123.3(-15.4)}$	I
<b>D7</b>	$\text{Col}_{\text{hp}}$	$\xleftarrow{116.6(-9.3)}$	$\text{Col}_{\text{h}}$
		$\xleftarrow{130.7(-11.6)}$	I
<b>D8</b>	$\text{Col}_{\text{hp}}$	$\xleftarrow{151.3(-33.7)}$	I
		$\xleftarrow{154.2(-29.3)}$	I
<b>D9</b>	$\text{Col}_{\text{hp}}$	$\xleftarrow{144.8}$	$\text{Col}_{\text{h}}$
		$\xleftarrow{146.7}$	I
<b>D10</b>	$\text{Col}_{\text{hp}}$	$\xleftarrow{130.6(-5.7)}$	$\text{Col}_{\text{h}}$
		$\xleftarrow{140.8(-16.3)}$	I
<b>D11</b>	$\text{Col}_{\text{hp}}$	$\xleftarrow{103.3(-3.2)}$	$\text{Col}_{\text{h}}$
		$\xleftarrow{125.8(-15.6)}$	I
<b>D12</b>	$\text{Col}_{\text{hp}}$	$\xleftarrow{103.3(-3.2)}$	$\text{Col}_{\text{h}}$
		$\xleftarrow{125.8(-15.6)}$	I

<sup>a</sup> Compound **D10** failed to be detected exact enthalpies since the transition peaks in its DSC curves are too close.

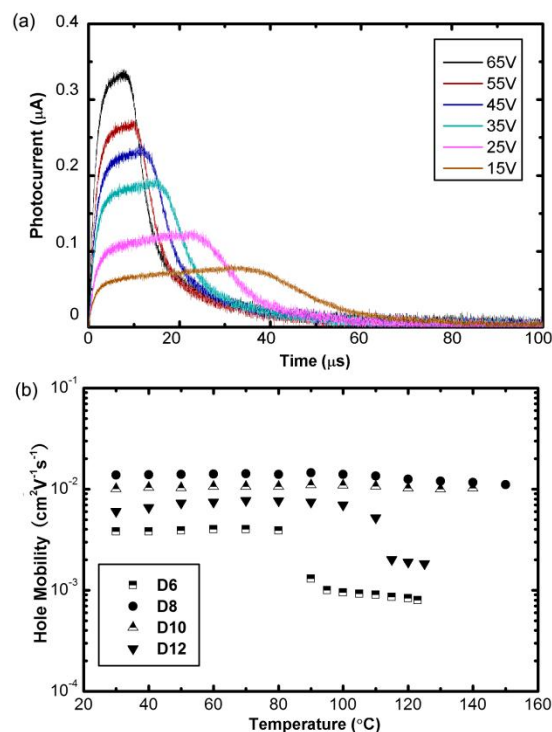


**Fig. 1** a) Typical TOF transits for **D6** at  $40\text{ }^{\circ}\text{C}$  and b) temperature dependences of hole mobilities of **D6**, **D8**, **D10** and **D12** at an applied electric field of  $2 \times 10^4\text{ V/cm}$ .

Charge carrier mobilities of compounds **D6-D12** were measured by a time-of-flight (TOF) method under controlled temperature. These compounds were capillary-filled into liquid crystal cells consisting of two ITO-coated glass surfaces at their isotropic temperatures. The cells were illuminated by a nitrogen gas laser ( $\lambda = 337$  nm) pulse with 10ns intervals. The photocurrent as a function of time were recorded by digital oscilloscope and analyzed in linear and double logarithmic plots. The transit time  $t_T$  was determined from the kink point in the transient photocurrent curves. The charge carrier mobility  $\mu$  is calculated according to eqn (1), where  $V$  is the applied voltage and  $d$  is the sample thickness.

$$\mu = d^2/Vt_T \quad (1)$$

Non-dispersive transient photocurrents for hole were observed in all these compounds **D6-D12**. In contrast to the case of the holes, weak featureless photocurrent signals were obtained for electrons and their mobility could not be determined. Fig. 1a exhibited transient photocurrent curves for hole in the  $\text{Col}_{\text{hp}}$  phase of compound **D6** at 40 °C. The hole mobility was calculated to be  $3.8 \times 10^{-3} \text{cm}^2 \text{v}^{-1} \text{s}^{-1}$ . The relationship between hole mobilities and the temperature of **D6** was shown in the Fig. 1b, mobilities in the higher temperature  $\text{Col}_{\text{h}}$  phase were observed a slightly negative dependence on temperature ( $8.3 \times 10^{-4} \text{cm}^2 \text{v}^{-1} \text{s}^{-1}$  at 120 °C and  $9.5 \times 10^{-4} \text{cm}^2 \text{v}^{-1} \text{s}^{-1}$  at 95 °C). When cooling from  $\text{Col}_{\text{h}}$  phase to  $\text{Col}_{\text{hp}}$  phase, a dramatic increase in mobility was observed near the transition point of **D6**, this result reflected the fact that  $\text{Col}_{\text{hp}}$  phase was more ordered than  $\text{Col}_{\text{h}}$  phase. Hole mobility in  $\text{Col}_{\text{hp}}$  phase of **D6** was independent to temperature, This weak temperature dependence of the mobilities combined with the non-dispersive Gaussian transient curves and the indicated the charge carrier transport as band transport model.<sup>12, 20</sup> Similar results were obtained in dimers **D7**, **D11** and **D12**, the hole mobilities of **D7** were located between **D6** and **D8**, while mobilities **D11** located between **D10** and **D12**. Hole mobilities of **D12** as a function of temperature in both their  $\text{Col}_{\text{h}}$  phase and  $\text{Col}_{\text{hp}}$  phase were also shown in Fig. 1b.

**D8**, **D9** and **D10** showed similar results when observed their charge carrier mobilities of columnar plastic phases as a function of temperature (Fig. 1b). Although a  $\text{Col}_{\text{h}}$  phase was observed in **D10** at its higher temperature range by DSC and POM (ESI Fig. 5,6), mobilities of this phase was failed to be measured out due to the short temperature range which required the temperature controlling to be more delicate. The mobilities of **D8**, **D9** and **D10** were independent on temperatures in a long temperature range and experienced slight decreases with increase of temperatures when close to their isotropic temperatures. The hole mobilities at the columnar plastic phases of **D8**, **D9** and **D10** can reach  $1.4 \times 10^{-2} \text{cm}^2 \text{v}^{-1} \text{s}^{-1}$ ,  $1.3 \times 10^{-2} \text{cm}^2 \text{v}^{-1} \text{s}^{-1}$  and  $1.1 \times 10^{-2} \text{cm}^2 \text{v}^{-1} \text{s}^{-1}$ , respectively.

Table 2 summarized hole mobilities of **D6-D12** in their  $\text{Col}_{\text{hp}}$  phases at 40 °C. Mobility of **D8** showed the maximum value, while those of other dimers decreased regularly both with linkage lengths becoming shorter or longer. The interesting phenomenon on charge carrier mobility was reported here for the first time and illustrated that linkage lengths played a significant role on the modulation of charge transport properties.

Charge carrier mobilities in discotic liquid crystals always influenced by their geometric fluctuations due to their one-dimensional conductivity natures.<sup>12, 13</sup> The changes in mobility may generally result from the different fluctuations in the stacking distances of molecules or lateral movements of the molecules within the same column.<sup>14, 15, 16</sup> For this type of dimers, in which both the free side chains and the linkages were

linked to the cores by ether bonds, the two subunits most likely to occupy neighbouring columns. Their freedom to reorient is restricted by the effect of the spacer which always resulted in high-amplitude lateral librations.<sup>17</sup> The [002], [102] peaks which presented the  $\pi$ - $\pi$  stacking of molecules in these dimers also showed no major differences and regular dependence on the linkage lengths (Table 2),<sup>9</sup> thus the changes in the mobilities of these dimers should generated by their different levels of lateral displacements within the molecular columns.

**Table 2** hole mobilities and stack distances in  $\text{Col}_{\text{hp}}$  phase of **D6-D12** at 40 °C with an applied electric field of  $2 \times 10^4$  V/cm

Compound	$\mu_{\text{h}} / \text{cm}^2 \text{v}^{-1} \text{s}^{-1}$	$d$ -spacing/Å	
		d(002)	d(102)
<b>D6</b>	$3.8 \times 10^{-3}$	3.55	3.47
<b>D7</b>	$6.0 \times 10^{-3}$	3.54	3.46
<b>D8</b>	$1.4 \times 10^{-2}$	3.53	3.47
<b>D9</b>	$1.2 \times 10^{-2}$	3.55	3.46
<b>D10</b>	$1.0 \times 10^{-2}$	3.54	3.46
<b>D11</b>	$9.3 \times 10^{-3}$	3.53	3.46
<b>D12</b>	$6.6 \times 10^{-3}$	3.54	3.46

In contrast with monomeric discotic molecules, lateral correlations due to steric perturbations between neighbouring columns were introduced in these dimers by their spacers.<sup>6, 7, 17, 25</sup> The lateral motions of the subunits of these dimers should be generated by steric perturbations and influenced by the linkage lengths. Compound **D8** has a “perfect twin” structure, for the length of linkage is twice of its free side chains, the perturbation was minimized because the structure of the mesophase can be visualized as columns consisting of stacked separated monomeric units **HAT4**.<sup>17</sup> Thus **D8** exhibited perfect properties in phase behaviour and charge mobility which closed to its corresponding monomer **HAT4**. We supposed that dimers with linkage lengths shorter or longer than twice the length of side chains, the perturbation appeared as strain or steric crowd, respectively. Lateral motion of discotic molecules increased due to the increasing of steric perturbations which resulted in different charge carrier mobilities. On the other hand, the increasing of steric perturbations decreased the stability of packing columns, thus promoted the formation lower ordered phases at higher temperature ranges.<sup>26</sup>

To confirm this investigation, we newly synthesized the corresponding monomers **M3-M6**. In contrast to their dimers **D6-D12**, these monomers can be visualized as the dimers being “halved” from their linkages. If the steric perturbations appeared in these dimers as described above, with the absence of linkage between neighbouring columns, a prediction of phase behaviours of **M3-M6** were easy to make. Monomer **M4** (**HAT4**), is exactly half of its dimer **D8** which has a “perfect twin” structure with minimized steric perturbation, the halving of linkage should have no influence on its phase behaviour, thus **M4** should exhibit a single  $\text{Col}_{\text{hp}}$  phase. For **M3**, the strain in its dimer **D6** was absent with the halving of linkage, so that the steric perturbation was disappear in the columnar phase of **M3**, coupling with the similarity in structure with **M4**, **M3** should also exhibit a single  $\text{Col}_{\text{hp}}$  phase. In **M5** and **M6**, the steric perturbation in their dimers **D10** and **D12** appeared as steric crowds which would not disappear even the restrictions

of linkages was cancelled, thus **M5** and **M6** should give the multiple phase behaviours which were similar to **D10** and **D12**.

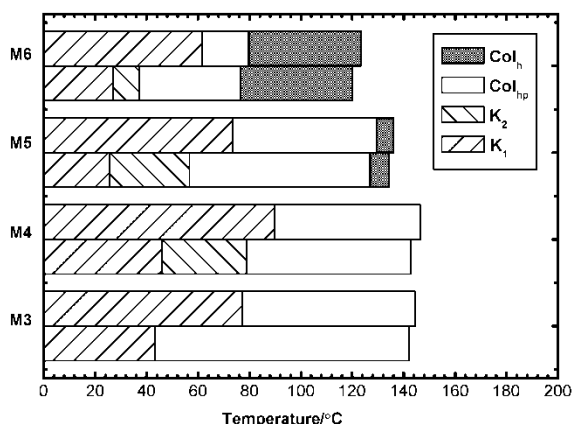


**Fig. 2** Graph of phase transition temperatures of **M3-M6** on heating (above column) and cooling (below column) runs. Transition temperatures were based on the 1<sup>st</sup> cooling runs and 2<sup>nd</sup> heating runs by DSC at 10 °Cmin<sup>-1</sup>. Phase assignments of **M3-M6** were based on observation of DSC, POM and XRD ( $K_1$ ,  $K_2$ , = crystalline phase).

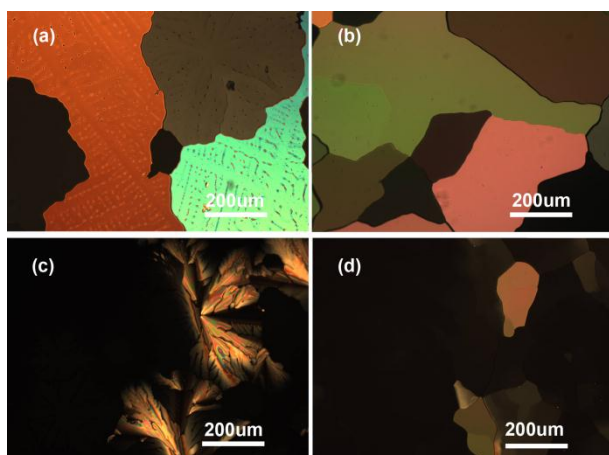


**Fig. 3** (a) mosaic texture for  $Col_{hp}$  phase of **M3** at 90 °C; (b) mosaic texture for  $Col_{hp}$  phase of **M4** at 120 °C; (c) dendritic texture for  $Col_h$  phase of **M5** at 135 °C; (d) mosaic texture for  $Col_{hp}$  phase of **M5** at 125 °C. (Magnification 100 ×)

Phase study results of **M3-M6** (Fig. 2) were consistent with our prediction. Compound **M3** and **M4** exhibited a single  $Col_h$  phase while **M5** and **M6** showed two liquid crystal phases with a higher temperature  $Col_h$  and a lower temperature  $Col_{hp}$  phase. **M4** has also been reported to exhibit a single  $Col_{hp}$  phase in previously. The texture of **M3** observed by POM was a typical mosaic texture which was exactly similar to that of  $Col_{hp}$  phase of **M4** (Fig. 3a, 3b). When heating powder samples into liquid crystal phase, **M3** also gave X-ray pattern which analogous to **M4**, two diffraction peaks in the wide-angle regime which was a signature of columnar plastic phase, and reflections in the small-angle regime should be originated from a hexagonal packing (Fig. 4a). Thus **M3** was confirmed to have a single  $Col_{hp}$  phase. The high temperature phases of **M5** and **M6** were identified as  $Col_h$  phase on the basis of the characteristic dendritic textures observed by POM (Fig. 3c). When they were

cooled into their lower temperature liquid crystal phases, the texture of **M6** did not show any changes while the texture of **M5** finally translated into mosaic texture (Fig. 3d). Similar XRD patterns of **M5** and **M6** which indicated clear phase transitions between two liquid crystal phases were obtained on cooling from isotropic phase. Single diffraction peak of approximately 3.6 Å in the wide-angle at the high temperature phase and the peak split into two reflections at low temperature range (Fig. 4b). Therefore, **M5** and **M6** were confirmed to have a high temperature  $Col_h$  and a low temperature  $Col_{hp}$  phase.

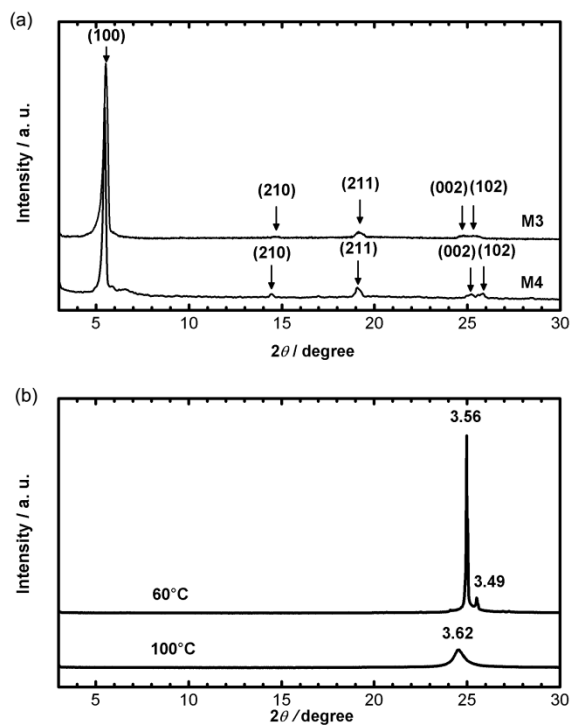


**Fig. 4** (a) XRD patterns for  $Col_{hp}$  phases of **M3** and **M4** on heating runs (**M3** at 120 °C and **M4** at 100 °C); (b) XRD patterns of **M6** at different temperatures on cooling runs ( $Col_{hp}$  at 60 °C and  $Col_h$  at 100 °C), the numbers were given by the corresponding Bragg distances in Å.

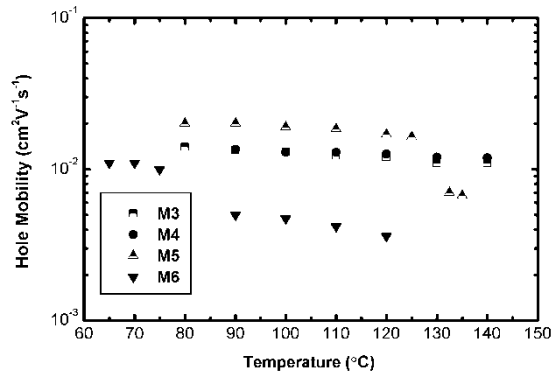


**Fig. 5** Temperature dependences of hole mobilities of **M3-M6** at an applied electric field of  $4 \times 10^4$  V/cm.

To further understand the influence of linkage length on charge carrier mobility of the dimer system, hole mobilities of these monomers **M3-M6** were investigated by TOF method with measurement condition similar to that of **D6-D12**. As shown in Fig. 5, **M3** and **M4** gave similar hole mobilities

( $1.3 \times 10^{-2} \text{cm}^2 \text{v}^{-1} \text{s}^{-1}$  for both of **M3** and **M4** at 100 °C) with slightly negative dependence on temperature. Compounds **M5** and **M6** with multiphase behaviours showed phase dependent charge carrier mobilities, hole mobilities in their  $\text{Col}_{\text{hp}}$  phase ( $2.0 \times 10^{-2} \text{cm}^2 \text{v}^{-1} \text{s}^{-1}$  for **M5** at 90 °C,  $1.1 \times 10^{-2} \text{cm}^2 \text{v}^{-1} \text{s}^{-1}$  for **M6** at 70 °C) were several times higher than that of  $\text{Col}_{\text{h}}$  phase ( $7.0 \times 10^{-3} \text{cm}^2 \text{v}^{-1} \text{s}^{-1}$  for **M5** at 133 °C,  $4.2 \times 10^{-3} \text{cm}^2 \text{v}^{-1} \text{s}^{-1}$  for **M6** at 110 °C).

When we make a general comparison of hole mobilities in  $\text{Col}_{\text{hp}}$  phase of **M3-M6** (Fig.5), the results of **M3**, **M4** and **M6** with a relationship of  $\mu_{\text{M3}} \approx \mu_{\text{M4}} > \mu_{\text{M6}}$  also consistent with our description on the existence of steric perturbation. After halving from their corresponding dimers, the strain was disappeared in **M3**, as a result, the lateral motion of discotic molecules within columns caused by it also been cancelled, thus gave the mobility similar to that of **M4**. In **M6**, the steric crowd in its dimers **D12** would not disappear after halving, so that the lateral motion still existent, therefore **M6** gave mobility smaller than **M4**. Although **M5** which was expected to give the mobility higher than **M4** and lower than **M6**, it showed higher mobility than both of them. This may be an imperfection of our interpretation about the relevance of linkage length in charge carrier mobilities of dimers. But a fact should be noted that XRD pattern in  $\text{Col}_{\text{hp}}$  phase of **M5** obtained on heating process gave unique diffractions which indicated a perfect homeotropic alignment (ESI Fig. 7).<sup>18-21</sup> Sharp and high intensity peak (100) was appeared at low angle region while the peaks at large angle region were absent. Furthermore, texture of **M5** observed by POM was easy to show large dark area when cooling into  $\text{Col}_{\text{hp}}$  phase from  $\text{Col}_{\text{h}}$  phase which also indicated a perfect homotropic alignment.<sup>20-21</sup> This may be a factor for its high charge carrier mobility, further study aimed at clarifying this point will be carried out in our future work.

A comparison on hole mobilities in  $\text{Col}_{\text{hp}}$  phase between dimers and their monomers also made based on our measurement results. In contrast to monomers **M3-M6**, dimers **D6**, **D10** and **D12** gave mobilities smaller than their corresponding monomers **M3**, **M5** and **M6**, while **D8** maintained mobility of **M4**. The introduction of linkage seems to have no effect on promoting charge carrier mobility of the dimer even though it was expected to stabilize the phase structure of monomer. In fact, based on our above investigation, linkage introduced steric perturbation which may decrease the stabilization of phase structures in these dimers. This perturbation was relative with linkage length. For **D8**, with the “perfect twin” structure, the perturbation was minimized because the structure of the mesophase can be visualized as columns consisting of stacked separated monomeric units **M4**, thus maintained the mobility of **M4**.<sup>17, 18</sup> Similar result has also been reported in the “perfect twin” of hexapentyloxytriphenylene (**HAT5**), which gave mobility similar to that of **HAT5**, neither hinders nor promotes.<sup>23, 24</sup> For **D6**, because the linkage length shorter than twice of side chains, the interaction of side chains caused a strain between neighbouring columns, which increased lateral motion of discotic molecules.<sup>7, 17, 26</sup> In **M3**, this strain was cancelled because the absent of linkage, thus **D6** gave mobility smaller than that of **M3**. For **D10** and **D12**, longer linkage introduced steric crowd also gave rise lateral motion. Even though the steric crowd still appeared in **M5** and **M6** after cancellation of restriction from linkage, the free rotations of the monomers about the columnar axis can help release part of this perturbation. These free rotations were limited in **D10** and **D12**

due to the restrictions of linkage, which lead to smaller mobilities.<sup>7, 17</sup>

Our work clearly illustrated the important role played by linkage length in modulation of charge carrier mobilities, as well as in molecular design of discotic liquid crystal dimers. The formation of dimer seems hardly to improve mobility of monomer because the introduction of steric perturbation, this may be also a reason that most of current discotic liquid crystal oligomers and polymers suffered low quality stacking structures and low mobilities. However, with excellent film making and mechanical properties, liquid crystal dimers, oligomers and polymers were still largely appealing in the field of material research for organic thin film devices. In this case, the molecular design strategy which can maintain charge carrier mobilities of their monomers (i. e. form a “perfect twin” structure in dimers) was needed to improve in these systems. For further understanding of the structure-properties in liquid crystal dimers, investigation on dimers formed by hexapentyloxytriphenylene (**HAT5**) and hexapropoxytriphenylene (**HAT3**) are in processing.

## Conclusions

Phase behaviours and charge carrier mobilities of a series of triphenylene-based dimers were systematically investigated. A clear structure-property relationship which has not been reported before was revealed in this study. Linkage length was demonstrated to play an important role in the modulation of phase behaviours and charge carrier mobilities in these dimers. In contrast with monomeric discotic molecules, a steric perturbation between the subunits embedded in neighbouring columns was introduced by the spacer in the formation of dimers. For compound **D8** with linkage exactly twice the length of its side chains, the perturbation was minimized thus it gave the best ordered phase behavior and the highest charge carrier mobilities. For the dimers with linkage chain shorter or longer than twice of the side chains, the perturbations appeared as strain or steric crowd, which result in different degree of lateral fluctuations of discotic moieties in neighbour columns and give rise to multiple phase behaviours and the differences in charge carrier mobilities. The phase behaviours and charge carrier mobilities of corresponding monomers consistently demonstrated the reasonability of the existence of steric perturbation. This work promoted us a clear understanding of the properties-structure relationship of discotic liquid crystals dimers and can also provide a molecular design strategy for discs dimers or polymers with controllable phase behaviour and predictable properties.

## Experimental section

All solvents employed were purchased from Aldrich and used without further purification unless stated otherwise. Column and thin layer chromatography were performed on silica gel 60 (200–300 mesh ASTM) and Silica Gel 60 glass backed sheets, respectively. <sup>1</sup>H-NMR spectra were measured in  $\text{CDCl}_3$  on Bruker NMR spectrometers (DMX 300 MHz), chemical shifts are given in parts per million ( $\delta$ ) and are referenced from tetramethylsilane (TMS). Multiplicities of the peaks are given as s = singlet, d = doublet, t = triplet, m = multiplet. Fourier transform infrared spectroscopy (FT-IR) were carried out on a Shimadzu FTIR-8400 spectrometer using KBr pellets. High resolution mass spectrum was recorded on a Bruker Apex IV FTMS mass spectrometer.

Polarising optical microscopy was carried out on an Leica DM4500P microscopy equipped with a Linkam TMS94 hot stage. Differential scanning calorimetry was carried out on a Netzsch DSC 200 at a heating and cooling rate of 10 °C min<sup>-1</sup>. X-Ray diffraction studies were conducted on a Bruker D8 Advance diffractometer equipped with variable temperature controller.

Charge mobility was measured by a time-of-flight device (TOF-401). The LC cells with the thickness of 15µm were purchased from E.H.C. company with the semi-transparent indium tin oxide (ITO) electrodes. The purified compounds were capillary-filled into the cell at the temperature 10 °C higher than their clear point, and then slowly cooling to their mesophases at a rate of 0.1 °C min<sup>-1</sup> in order to obtain a well-defined homeotropic alignment. The cell was placed on the hotstage and illuminated by light pulses from a N<sub>2</sub> laser (USHO KEC 160, wavelength 337 nm, pulse width is 600ps). The transient photocurrent across the cell was amplified using a NF low-noise current preamplifier (model 5307) and monitored using a digital phosphor oscilloscope (Tektronix TDS 3032C). The bias voltage was applied to the sample with a power supply unit (Kikusui PAN110-3A). Measurements above room temperature were carried out under atmosphere.

Compounds **D6-D12**, **M4** were synthesized without any change according to our previously reported work.<sup>8</sup> Compounds **M3**, **M5** and **M6** were synthesized from 2-hydroxy-3,6,7,10,11-pentabutyloxytriphenylene and the appropriate 1-bromoalkane.<sup>27, 28</sup> The products were purified with flash chromatography and recrystallized from ethanol and n-hexane several times.

#### General synthesis of M3, M5 and M6

A mixture of 2-hydroxy-3,6,7,10,11-pentabutyloxytriphenylene (500mg), 1-Bromoalkane (1.2 eq.) and anhydrous potassium carbonate (0.5g) in ethanol (20ml) was heated under reflux for 24h. The mixture was cooled to 0 °C, filtered, washed with water (50ml), and extracted with dichloromethane (2 × 50ml), the solvent removed in vacuo, and the residue purified by column chromatography on silica eluting with dichloromethane and finally recrystallized from ethanol and n-hexane several times to give pure **M3**, **M5** and **M6**.

**2-propoxy-3,6,7,10,11-pentabutyloxytriphenylene M3** (0.3g, 56%); IR (KBr):  $\nu_{\max}/\text{cm}^{-1}$  1261 (C-O-C);  $\delta_{\text{H}}$  (300MHZ, CDCl<sub>3</sub>) 7.85 (6H, m, ArH), 4.18-4.27 (12H, t, OCH<sub>2</sub>), 1.89-2.01 (12H, m, OCH<sub>2</sub>CH<sub>2</sub>), 1.52-1.68 (10H, m, OCH<sub>2</sub>CH<sub>2</sub>CH<sub>2</sub>), 1.03-1.17 (18H, m, CH<sub>3</sub>); HRMS (ESI): calc. m/z 647.4306 (C<sub>41</sub>H<sub>59</sub>O<sub>6</sub>), found m/z 647.4294 (M)<sup>+</sup>.

**2-pentyloxy-3,6,7,10,11-pentabutyloxytriphenylene M5** (0.53g, 95%); IR (KBr):  $\nu_{\max}/\text{cm}^{-1}$  1265 (C-O-C);  $\delta_{\text{H}}$  (300MHZ, CDCl<sub>3</sub>) 7.85 (6H, m, ArH), 4.23-4.27 (12H, t, OCH<sub>2</sub>), 1.91-1.96 (12H, m, OCH<sub>2</sub>CH<sub>2</sub>), 1.56-1.65 (12H, m, OCH<sub>2</sub>CH<sub>2</sub>CH<sub>2</sub>), 1.42-1.50 (2H, m, OCH<sub>2</sub>CH<sub>2</sub>CH<sub>2</sub>CH<sub>2</sub>), 0.96-1.11 (18H, m, CH<sub>3</sub>); HRMS (ESI): calc. m/z 675.4619 (C<sub>43</sub>H<sub>65</sub>O<sub>6</sub>), found m/z 675.4603 (M)<sup>+</sup>.

**2-hexyloxy-3,6,7,10,11-pentabutyloxytriphenylene M6** (0.54g, 94%); IR (KBr):  $\nu_{\max}/\text{cm}^{-1}$  1263 (C-O-C);  $\delta_{\text{H}}$  (300MHZ, CDCl<sub>3</sub>) 7.85 (6H, m, ArH), 4.23-4.27 (12H, t, OCH<sub>2</sub>), 1.89-1.98 (12H, m, OCH<sub>2</sub>CH<sub>2</sub>), 1.60-1.68 (12H, m, OCH<sub>2</sub>CH<sub>2</sub>CH<sub>2</sub>), 1.40-1.41 (4H, m, OCH<sub>2</sub>CH<sub>2</sub>CH<sub>2</sub>CH<sub>2</sub>CH<sub>2</sub>), 0.94-1.08 (18H, m, CH<sub>3</sub>); HRMS (ESI): calc. m/z 689.4776 (C<sub>44</sub>H<sub>65</sub>O<sub>6</sub>), found m/z 689.4759 (M)<sup>+</sup>.

#### Acknowledgements

This work is support by the fund from Beijing Municipal Education Commission Project (Grant NO. KM201110015003, Grant NO. KM201210015008, NO.Byyc201316-007), the Importation and Development of High Caliber Talents Project of Beijing Municipal Institutions (CIT&TCD201304123), the Key (Key grant)Project of Chinese Ministry of Education [grant number 211004].

#### Notes and references

Information Recording Materials Lab, Lab of Printing & Packaging Material and Technology, Beijing Institute of Graphic Communication, 102600 Beijing, China. Fax: 86-10-60261108; Tel: 86-10-60261110; E-mail: zhangchunxiu@bigc.edu.cn

† Footnotes should appear here. These might include comments relevant to but not central to the matter under discussion, limited experimental and spectral data, and crystallographic data.

Electronic Supplementary Information (ESI) available: Experimental data, synthesis, characterization, polarized optical microscopy, thermal analysis. See DOI: 10.1039/b000000x/

- R. J. Bushby and O. R. Lozman, *Curr. Opin. Solid State and Mater. Sci.*, 2002, **6**, 569-578.
- H. Wu, C. Zhang, J. Pu and Y. Wang, *Liq. Cryst.*, 2014, **41**, 1173-1178.
- N. Boden, R. J. Bushby, and A. N. Cammidge, *J. Am. Chem. Soc.*, 1995, **117**, 924-921.
- C. Destrade, P. Foucher, H. Gasparoux, N. H. Tinh, A. M. Levelut and J. Malthete, *Mol. Cryst. Liq. Cryst.*, 1984, **106**, 121-146.
- S. Kumar, *Liq. Cryst.*, 2005, **32**, 1089-1113.
- N. Boden, R. J. Bushby, A. N. Cammidge, A. E. Mansoury, P. S. Martin and Z. Lu, *J. Mater. Chem.*, 1999, **9**, 1391-1402.
- S. Zamir, E. J. Wachtel, H. Zimmermann, S. Dai, N. Spielberg, R. Poupko and Z. Luz, *Liq. Cryst.*, 1997, **23**, 689-698.
- Y. Wang, C. Zhang, H. Wu and J. Pu, *J. Mater. Chem. C.*, 2014, **2**, 1667-1674.
- B. Glisen, W. Heitz, A. Kettner and J. H. Wendorff, *Liq. Cryst.*, 1996, **20**, 627-633.
- B. Glisen, A. Kettner and J. H. Wendorff, *Mol. Cryst. Liq. Cryst.*, 1997, **303**, 115-120.
- J. Simmerer, B. Glisen, W. Paulus, A. Kettner, P. Schuhmacher, D. Adam, K. H. Eitzbach, K. Siemensmeyer, J. H. Wendorff, H. Ringsdorf, D. Haarer, *Adv. Mater.*, 1996, **8**, 815-819.
- W. Pisula, M. Zorn, J. Y. Chang, K. Müllen and R. Zentel, *Macromol. Rapid Commun.*, 2009, **30**, 1179-1202.
- CY. Liu, HL. Pan, H. Tang, M. A. Fox, and A. J. Bard, *J. Phys. Chem.*, 1995, **99**, 7632-7636.
- D. L. Cheung and A. Troisi, *Phys. Chem. Chem. Phys.*, 2008, **10**, 5941-5952.
- J. J. Cornil, V. Lemaury, J. P. Calbert and J. L. Brédas, *Adv. Mater.*, 2002, **14**, 726-729.
- V. Lemaury, D. A. daSilvaFilho, V. Coropceanu, M. Lehmann, Y. Geerts, J. Piris, M. G. Debije, A. M. vandeCraats, K. Senthilkumar, L. D. A. Siebbeles, J. M. Warman, J. L. Bredas and J. Cornil, *J. Am. Chem. Soc.*, 2004, **126**, 3271-3279.
- S. Zamir, R. Poupko, Z. Luz, B. Hüsler, C. Boeffel, H. Zimmermann, *J. Am. Chem. Soc.*, 1994, **116**, 1973-1980.

- 18 W. Pisula, Ž. Tomović, B. E. Hamaoui, et al. *Advanced Functional Materials.*, 2005, **15**, 893-904.
- 19 X. Feng, W. Pisula, L. Zhi, et al. *Angewandte Chemie.*, 2008, **120**, 1727-1730.
- 20 H. Duran, B. Hartmann-Azanza, M. Steinhart, et al. *ACS nano.*, 2012, **6**, 9359-9365.
- 21 J. Kopitzke, J. H. Wendorff, B. Glisen. *Liquid Crystals.*, 2000, **27**, 643-648.
- 22 W. Kranig, B. Hüser, H. W. Spiess, et al. *Advanced Materials.*, 1990, **2**, 36-40.
- 23 D. Adam, F. Closs, T. Frey, et al. *Physical review letters.*, 1993, **70**, 457-460.
- 24 D. Adam, P. Schuhmacher, J. Simmerer, et al. *Advanced Materials.*, 1995, **7**, 276-280.
- 25 N. Tchegbotareva, X. Yin, M. D. Watson, P. Samorì J. P. Rabe and K. Müllen, *J. Am. Chem. Soc.*, 2003, **125**, 9734-9739.
- 26 Y. Miyake, A. Fujii, M. Ozaki, Y. Shimizu. *Synthetic Met.*, **159**, 875-879.
- 27 N. Boden, R. C. Borner, R. J. Bushby, A. N. Carnmidge and M. V. Jesudason, *Liq. Cryst.*, 1993, **15**, 851-858.
- 28 S. Kumar and M. Manickam, *Synthesis.*, 1998, **8**, 1119-1122.